Chinese Chemical Letters 31 (2020) 3209–3212

Contents lists available at ScienceDirect

Chinese Chemical Letters

journal homepage: www.elsevier.com/locate/cclet

Communication

A facile synthesis of non-aqueous $LiPO_2F_2$ solution as the electrolyte additive for high performance lithium ion batteries

Weimin Zhao[a,b], Fucheng Ren[b], Qizhang Yan[c], Haodong Liu[c,*], Yong Yang[b,*]

[a] College of Chemical Engineering and Safety, Binzhou University, Binzhou 256503, China
[b] State Key Laboratory for Physical Chemistry of Solid Surfaces, and Department of Chemistry, College of Chemistry and Chemical Engineering, Xiamen University, Xiamen 361005, China
[c] Department of Nanoengineering, University of California San Diego, La Jolla 92093, United States

ARTICLE INFO

Article history:
Received 5 April 2020
Received in revised form 30 April 2020
Accepted 7 May 2020
Available online 14 May 2020

Keywords:
Lithium difluorophosphate ($LiPO_2F_2$) solution
Electrolyte additives
Electrode-electrolyte interface
Synthesis
Li-ion batteries

ABSTRACT

Constructing a reliable and favorable electrode-electrolyte interface is crucial to utilize the exceptional energy storage capability in commercial lithium-ion batteries. Here, we report a facile synthesis approach for the lithium difluorophosphate ($LiPO_2F_2$) solution as an effective film-forming additive *via* direct adding the Li_2CO_3 into $LiPF_6$ solution at 45 °C. Benefiting from the significantly reduced interface resistance (R_{SEI}) and charge transfer impedance (R_{ct}) of both the cathode and anode by adding the prepared $LiPO_2F_2$ solution into a baseline electrolyte, the cycling performance of the graphite||$LiNi_{0.5}Mn_{0.3}Co_{0.2}O_2$ pouch cell is remarkably improved under all-climate condition.

The Nobel Prize in Chemistry 2019 rewards the development of the lithium-ion batteries (LIBs). The LIBs are not only being widely used in mobile devices, but also their markets for electric vehicles are rapidly growing [1]. However, when batteries are charged at high rates, various polarizations such as the resistance between electrode/electrolyte will result in limited utilization of active materials, increased propensity for Li dendrite [2]. It is important to design a (electro)chemically stable and ionically conductive passivating layer that prevents further electrolyte decomposition on the electrodes [3].

One of the attractive methods to form a stable passivating layer is to incorporate a small dosage of a foreign molecule into the bulk electrolytes [4]. Most of the interface film-forming electrolyte additives are unsaturated organic compounds. The polymers that generated from the preferential oxidation or reduction of the unsaturated compound participate the formation of interfacial films [5]. Although the organic additives protect anode or cathode *via* suppressing the decomposition of electrolyte, the high rate and the low temperature performance of the batteries are sacrificed [6,7].

Recently, lithium-salt-type compounds are proposed as additives for LIBs, which can form stable solid electrolyte interfaces (SEI) on both anode and cathode [8–11]. Previous studies have clarified that lithium difluorophosphate ($LiPO_2F_2$) contribute to the formation a conductive and stable CEI/SEI film on the surface of the electrode to improve both high temperature and low temperature performance of the cell [12–15]. Although the effects of $LiPO_2F_2$ additive on the performance of LIBs have been reported by a few groups, its synthesis has rarely been discussed yet. Moreover, the poor solubility of $LiPO_2F_2$ in the electrolyte limits it as functional additive in the commercial LIBs [16]. In this work, the $LiPO_2F_2$ solution was firstly prepared by a facile synthesis method using Li_2CO_3 and $LiPF_6$ as the raw materials mixing in dimethyl carbonate (DMC) solvent *via* one step reaction. With the addition of $LiPO_2F_2$ in the electrolyte, a 1.6 Ah graphite||$LiNi_{0.5}Mn_{0.3}Co_{0.2}O_2$ pouch cells shows superior cycling stability under all-climate condition. In addition, details of the evolutions of $LiPO_2F_2$ at different cycling process were further investigated by ion chromatography. A certain amount of alkyl phosphatesis generated accompanied by the consumption of $LiPO_2F_2$ in the electrolyte, indicating that $LiPO_2F_2$ decomposed and participated the formation of interface layer on the electrode surface, thus endowing the battery with enhanced performance and stability.

Since the $LiPF_6$ undergoes complete dissociation in dilute carbonate-based electrolytes to form coordinated Li^+ and uncoordinated PF_6^-, its carbonate solution exhibits high ionic

* Corresponding authors.
E-mail addresses: haodong.liu.xmu@gmail.com (H. Liu), yyang@xmu.edu.cn (Y. Yang).

https://doi.org/10.1016/j.cclet.2020.05.006
1001-8417/

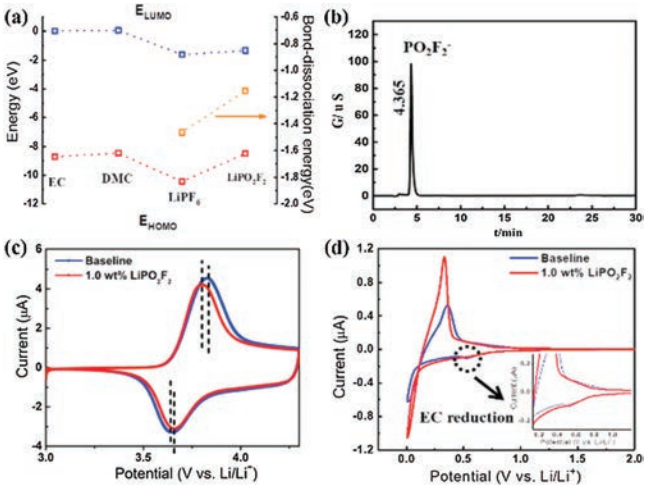

Fig. 1. (a) The highest occupied molecular orbital (HOMO) and the lowest unoccupied molecular orbital (LUMO) energies of the lithium salts ($LiPO_2F_2$ and $LiPF_6$) and solvents (EC, DMC). (b) IC chromatogram of $LiPO_2F_2$ solution reaction at 45 °C. (c) Cyclic voltammetric profiles of Li||NMC532 cell in the electrolytes with or without $LiPO_2F_2$, scan rate 0.2 mV/s. (d) Cyclic voltammetric profiles of Li||graphite cells in the electrolytes with or without $LiPO_2F_2$, scan rate 0.2 mV/s.

conductivity [4]. Fig. 1a compares the calculated dissociation energy of $LiPF_6$ and $LiPO_2F_2$. The higher dissociation energy of the $LiPO_2F_2$ indicates that $LiPO_2F_2$ is more difficult to dissociate in non-aqueous solvent than the $LiPF_6$. Experimentally, 1.0–3.0 wt% of $LiPF_6$ and $LiPO_2F_2$ powders are separately added into the ethylene carbonate/dimethyl carbonate (EC/DMC). As shown in Fig. S1 (Supporting information), the $LiPF_6$ is completely dissolved into the solvents and forms a transparent mixture in less than one minute. In contrast, the $LiPO_2F_2$ and the carbonate solvent forms at urbid mixture even after stirring for 3 h. Therefore, the dissolution of small amount of $LiPO_2F_2$ into the commercial electrolyte is a practical challenge. To address this problem, a one-step reaction is designed to synthesis the $LiPO_2F_2$ solution *via* direct adding the Li_2CO_3 into the $LiPF_6$-DMC solution (Reaction 1). The side product LiF is removed *via* vacuum suction filtration. The reaction temperature is conducted at 25 °C, 45 °C and 65 °C, respectively.

$$LiPF_6 + 2Li_2CO_3 \rightarrow LiPO_2F_2 + 4LiF\ (s) + 2CO_2\ (g) \quad (1)$$

The solution after reaction at different temperature is analyzed by ion chromatography (Fig. S2 in Supporting information). As show in Fig. S2a, there is no obvious formation of $LiPO_2F_2$ when the reaction temperature at 25 °C. However, when the reaction temperature increases to 65 °C (Fig. S2c), an obvious impurity peak at 10.413 min indicating the side reactions begin to occur. One possibility is that $LiPF_6$ has poor thermal stability and decomposes in organic solvent at elevated temperature, resulting in the formation of by-products [17].

The purity of $LiPO_2F_2$ solution synthesis at 45 °C also has been characterized *via* IC and NMR spectroscopy. A single peak characteristic of the product was observed at 4.833 min in the IC spectroscopy, which belong to $PO_2F_2^-$ singlet (Fig. 1b). As shown in Fig. S3a (Supporting information), there are three triplets at δ_P = −24.1 ppm, -17.6 ppm and -12.1 ppm in ^{31}P NMR spectroscopy [18]. From the structural formula of $PO_2F_2^-$, the F atom will split the directly bonded P atom, which is in accordance with the N + 1 rule, so a set of symmetrical triple peaks should be obtained in the ^{31}P NMR spectrum. The ^{19}F NMR spectrum provides additional support of pure compound with a symmetrical two doublets appear at the position of -78.73 ppm and -81.29 ppm, respectively. The IC and NMR spectra are consistent with high purity of $LiPO_2F_2$ solution.

Thermodynamically, the electrochemical redox potential of a lithium salt or solvent is closely related to its highest occupied molecular orbital (HOMO) and lowest unoccupied molecular orbital (LUMO) energy, a higher value of HOMO/LUMO typically indicates that a chemical can be oxidized/reduced at a lower voltage [19]. Cyclic voltammetry (CV) is a widely accepted method to investigate the oxidative/reductive stability of an electrolyte and the redox reactions of electrodes [20]. Fig. 1c shows a pair of redox peaks of the NMC532, representing the lithium insertion/extraction processes. A slight decreased polarization of cathode redox peaks is observed for the cell with electrolyte containing $LiPO_2F_2$ solution, which is consistent with the reduced interfacial impedance (Fig. S4a in Supporting information). Moreover, $LiPO_2F_2$ has lower LUMO energy than solvents EC and DMC, which indicates that the $LiPO_2F_2$ is reduced prior to the solvent. Fig. 1d shows that the incorporation of $LiPO_2F_2$ decreased the reduction peak current at approximately 0.6 V of bulk electrolyte during the initial charging process, which corresponds to the EC reduction. Moreover, the $LiPO_2F_2$ additive also reduces interfacial impedance at the anode (Fig. S4b in Supporting information).

The ionic conductivities of the bulk electrolyte and interfacial film are two important parameters that quantify how mobile (and available) the lithium ions are for the ongoing electrochemical reactions on both anode and cathode [21]. These conductivities also dictate the power density output of the cell. As shown in Fig. 2a, the ionic conductivity of the $LiPO_2F_2$ electrolyte decreases from 9.2 mS/cm to 8.4 mS/cm at room temperature. When the temperature drops to the melting point of the solvent (36.4 °C for EC and 4.6 °C for DMC), such as 0 °C and even to -25 °C [22], the ionic conductivities of bulk electrolytes drop from 5.1 mS/cm to 1.8 mS/cm. The ionic conductivities of the $LiPO_2F_2$ electrolyte is still slightly lower than that of the baseline electrolyte at -25 °C. Although the addition of $LiPO_2F_2$ slightly decreases the ionic conductivity of bulk electrolyte, after three formation cycles, the R_{ct} and R_{SEI} of the cell using the baseline electrolyte are two times larger than the cell with $LiPO_2F_2$ (Fig. S5 in Supporting information). These results indicating $LiPO_2F_2$ can significantly modifies the interface layers and leads to much lower R_{ct} and R_{SEI} on both electrodes.

Fig. 2b compares room temperature cycling performance of 1.6 Ah graphite||NMC532 pouch cells using different electrolytes, namely, baseline 1.0 mol/L $LiPF_6$/EC-DMC (named BE), electrolyte

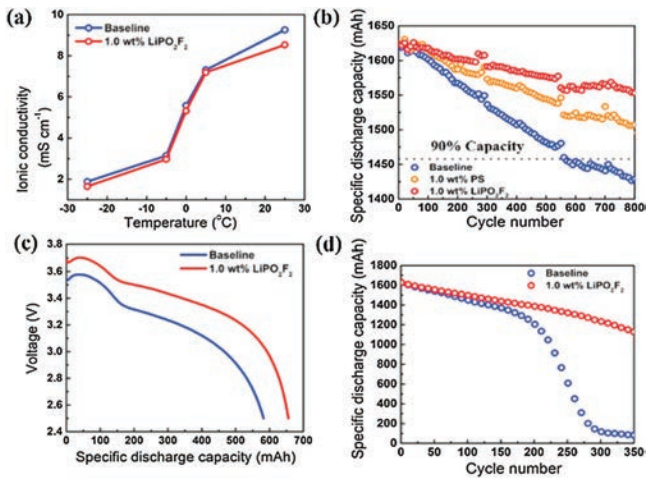

Fig. 2. (a) Ionic conductivities of baseline and containing $LiPO_2F_2$ electrolyte at different temperatures. (b) Discharge capacities of graphite||NMC532 cells with different electrolytes after 800 cycles at 25 °C. (c) Discharge voltage profile of graphite||NMC532 cells under 0.2 C rate at -25 °C. (d) Cycling stability of graphite|| NMC532 cells under 1.0 C at 45 °C after a -25 °C discharge process.

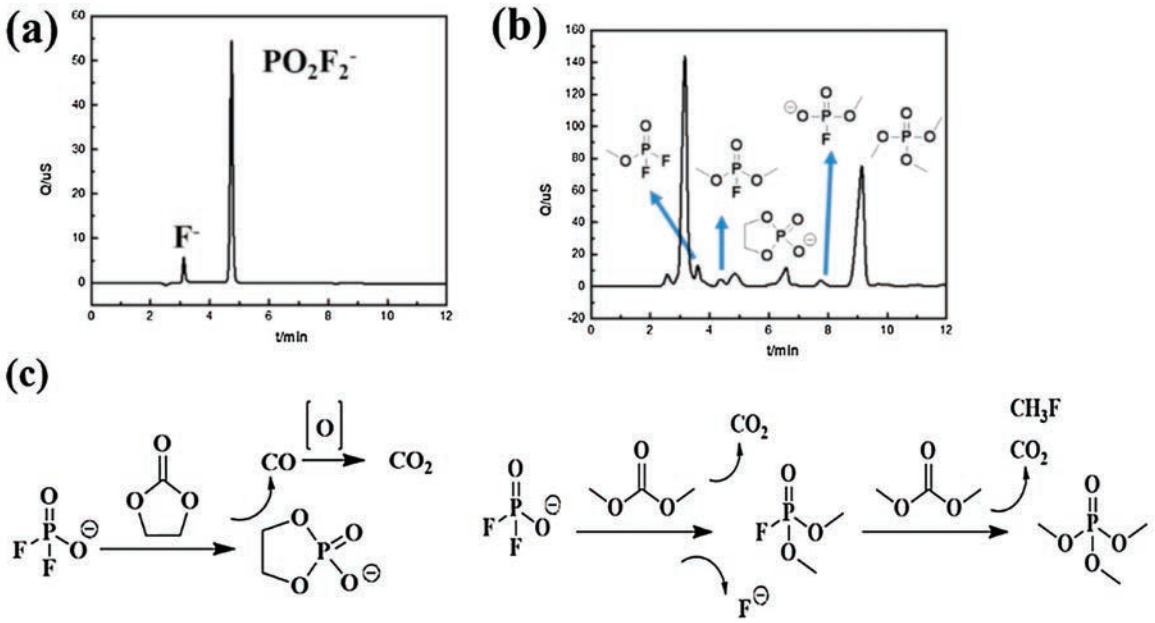

Fig. 3. IC chromatograms of the 1.0 wt% $LiPO_2F_2$ electrolyte, the electrolyte was extracted from the graphite||NMC532 pouch cells. (a) After the formation process; (b) After 350cycles; (c) Proposed degradation mechanisms of $LiPO_2F_2$ in organic carbonatebase electrolytes.

with 1.0 wt% PS (named PS1), and electrolyte with $LiPO_2F_2$ solution (named LiDFP1). After 800 cycles at 1 C, the capacity retention of the BE cells, PS1cells, and LiDFP1 cells are 88.1%, 92.8% and 95.7%, respectively. An appreciable capacity fading appears for the cells cycled in the BE electrolyte. This decay is mainly caused by the electrolyte decompositions on both anode and cathode [23]. With the interface films constructed by $LiPO_2F_2$, the graphite||NMC532 pouch cell cycled in the $LiPO_2F_2$-containing electrolytes shows much better cycling stability and more stable coulombic efficiencies (Fig. S6 in Supporting information) than those cycled in the BE and the PS electrolytes. Since adding an additive into the electrolyte does not bring extra step during the manufacturing of LIBs, the effectiveness of the $LiPO_2F_2$ solution provides a practical approach for enhancing the performance of current commercial LIBs at low cost.

The addition of the $LiPO_2F_2$ to the BE electrolyte also boosts the discharge capacity of graphite||NMC532 pouch cell at low temperature. The cell retains a high capacity of 665 mAh under 0.2 C rate at -25 °C, corresponding to 59% capacity retention. While the BE cell delivers a much lower capacity of 584 mAh. More importantly, the LiDFP1 cell exhibits 200 mV higher discharge middle plateau than the BE cell (Fig. 2c), implying that the interface layer modified by the $LiPO_2F_2$ is highly conductive for Li^+ transportation. The performance of graphite||NMC532 cells using different electrolytes was further investigated at an elevated temperature (45 °C) after the -25 °C discharge process. The BE cell shows inferior cyclability at 45 °C (Fig. 2d). For the BE electrolyte, an increase in the testing temperature drastically accelerates the parasitic reactions of POF_3 and HF with electrolyte [24]. They deteriorate the stability of interface layers that protect the electrodes upon cycling, resulting in the dissolution of transition metal ions at the cathode surface and the decomposition of electrolyte [25]. This ultimately leads to fast capacity decay observed at around 185th cycle. Its capacity drops to only 82 mAh after 350 cycles. Therefore, graphite||NMC532 cell with baseline electrolyte shows a shortened cycle life at 45 °C. In contrast, the LiDFP1 cell still delivers 1127 mAh at the 350th cycle, which corresponds to 69.3% of its initial capacity. The $LiPO_2F_2$ is able to mitigate the side reactions that destroy the interfacial film, which is beneficial for the high temperature cycling stability [26]. The electrochemical tests demonstrate that the electrolyte with $LiPO_2F_2$ drastically improves the performance of graphite|| NMC532 pouch cells at both low temperature discharge process and elevated temperature cycling.

IC chromatograms are conducted on the electrolytes extracted from the graphite||NMC532 pouch cells to track the evolutions of $LiPO_2F_2$ after the formation process and 350th cycles. It can be concluded that $LiPO_2F_2$ participates and forms certain amount of F^- in the interfacial chemistry on graphite anode and NMC532 cathode at formation cycle (Fig. 3a), despite the absence of $LiPO_2F_2$ redox decomposition peaks in the corresponding CV curves. Furthermore, the corresponding IC chromatogram obtained from the same electrolyte after 350th cycles at elevated temperature is shown in Fig. 3b, the analytes are alkyl phosphates [27,28]. None of the analyzed ionic compounds are available as a standard. The proposed degradation mechanisms of $LiPO_2F_2$ in organic carbonate base electrolytes are plotted in Fig. 3c. The formation of ionic compounds is a two-step reaction, based on a subsequent substitution of –F group in $PO_2F_2^-$ by $-OCH_3$ or $-OCH_2CH_2O-$ groups from the DMC or EC and concomitant decarboxylation. The combination of organic carbonate solvent and $LiPO_2F_2$ complement each other in restricting excessive additive consumption, which assists the growth of interphase and mitigates cell impedance increases.

In summary, a $LiPO_2F_2$ solution has been prepared and investigated as film forming additive for lithium ion pouch cells. The high purity $LiPO_2F_2$ solution can be generated *via* the reaction of $LiPF_6$ and Li_2CO_3 in dimethyl carbonate at 45 °C. Incorporation of $LiPO_2F_2$ solution into 1.0 mol/L $LiPF_6$ baseline electrolyte results in remarkably improved capacity retentions for 1.6 Ah graphite|| NMC532 pouch cells under all-climate condition.This work provides a novel, effective and viable approach that can be directly applied to the current production of LIBs.

Declaration of competing interest

The authors declare no competing financial interest.

Acknowledgments

We would like to acknowledge that this work is financially supported by National Natural Science Foundation of China (Nos. 21935009, 21761132030 and 21621091), National Key Research and Development Program of China (No. 2018YFB0905400) and the Doctoral Research Foundation of Binzhou University (No. 2016Y06).

Appendix A. Supplementary data

Supplementary material related to this article can be found, in the online version, at doi:https://doi.org/10.1016/j.cclet.2020.05.006.

References

[1] M. Li, J. Lu, Z.W. Chen, et al., Adv. Mater. 30 (2018) 1800561.
[2] Y.Y. Liu, Y.Y. Zhu, Y. Cui, Nat. Energy 4 (2019) 540–550.
[3] Y. Yu, P. Karayaylali, Y. Katayama, et al., J. Phys. Chem. C 122 (2018) 27368–27382.
[4] K. Xu, Chem. Rev. 114 (2014) 11503–11618.
[5] W. Zhao, Y. Ji, Z. Zhang, et al., Curr. Opin. Electrochem. 6 (2017) 84–91.
[6] J. Xia, L. Madec, L. Ma, J. Power Sources 295 (2015) 203–211.
[7] W.M. Zhao, B.Z. Zheng, H.D. Liu, et al., Nano Energy 63 (2019) 103815.
[8] M.Q. Xu, L. Zhou, Y.N. Dong, et al., Energy Environ. Sci. 9 (2016) 1308–1319.
[9] Y.C. Li, S. Wan, G.M. Veith, et al., Adv. Energy Mater. 7 (2017) 1601397.
[10] J. Cha, J.G. Han, J. Hwang, et al., J. Power Sources 357 (2017) 97–106.
[11] X.Q. Zhang, T. Li, B.Q. Li, et al., Angew. Chem. Int. Ed. 59 (2020) 3252–3257.
[12] J.W. Chen, L.D. Xing, X.R. Yang, et al., Electrochim. Acta 290 (2018) 568–576.
[13] Y. Chen, W.M. Zhao, Q.H. Zhang, et al., Adv. Funct. Mater. (2020) 2000396.
[14] M.F. He, R. Gao, M. Hobold, et al., Proc. Natl. Acad. Sci. U. S. A. 117 (2020) 73–79.
[15] Y.K. Li, B. Cheng, F.P. Jiao, et al., ACS Appl. Mater. Interfaces 12 (2020) 16298–16307.
[16] W.M. Zhao, G.R. Zheng, M. Lin, J. Power Sources 380 (2018) 149–157.
[17] J.G. Han, K. Kim, Y. Lee, et al., Adv. Mater. 31 (2019) 1804822.
[18] E. Markevich, R. Sharabi, H. Gottlieb, et al., Electrochem. Commun. 15 (2012) 22–25.
[19] K. Leung, C.M. Tenney, J. Phys. Chem. C 117 (2013) 24224–24235.
[20] X. Yu, A. Manthiram, Energy Environ. Sci. 11 (2018) 527–543.
[21] B. Liao, H. Li, M. Xu, et al., Adv. Energy Mater. 8 (2018) 1800802.
[22] E.R. Logan, E.M. Tonita, K.L. Gering, et al., J. Electrochem. Soc. 165 (2018) A21–A30.
[23] J.M. Zheng, M.H. Engelhard, D. Mei, et al., Nat. Energy 2 (2017) 17012.
[24] A.M. Haregewoin, A.S. Wotango, B.J. Hwang, Energy Environ. Sci. 9 (2016) 1955–1988.
[25] J.M. Tarascon, M. Armand, Nature 414 (2001) 359–367.
[26] J. Kim, J. Lee, H. Ma, et al., Adv. Mater. (2017) 1704309.
[27] Y.P. Stenzel, J. Henschel, M. Winter, et al., RSC Adv. 20 (2019) 11413–11419.
[28] W. Weber, R. Wagner, B. Streipert, J. Power Sources 306 (2016) 193–199.